

IIB matrix model: Extracting spacetime points

F.R. Klinkhamer*

*Institute for Theoretical Physics,
Karlsruhe Institute of Technology (KIT),
76128 Karlsruhe, Germany*

Abstract

Assuming that the large- N master field of the Lorentzian IIB matrix model has been obtained, we go through the procedure of how the coordinates of emerging spacetime points can be extracted. Explicit calculations with test master fields suggest that the genuine IIB-matrix-model master field may have a fine-structure that is essential for producing the spacetime points of an expanding universe.

PACS numbers: 98.80.Bp, 11.25.-w, 11.25.Yb

Keywords: origin and formation of the Universe, strings and branes, M theory

* frans.klinkhamer@kit.edu

I. INTRODUCTION

The IIB matrix model [1, 2] has been studied numerically in its Lorentzian version [3–5]. But how, conceptually, a classical spacetime emerges in Refs. [1–5] was unclear.

It has been suggested, in App. B of Ref. [6], that the large- N master field must play a crucial role for the emergence of a classical spacetime. As a follow-up, Ref. [7] presented an explicit (coarse-graining) procedure for extracting classical spacetime from the master field.

Here, we give some numerical results to illustrate the procedure of Ref. [7], as regards the extraction of the spacetime points (the extraction of a spacetime metric is more difficult and will not be discussed here). First, we consider a test master field with randomized entries on a band diagonal and, then, we consider a specially designed test master field with a deterministic fine-structure, which gives rise to multiple strands of spacetime that appear to fill out an expanding universe. This last type of test master field provides an *existence proof* that there can be master fields for which the procedure of Ref. [7] produces more or less acceptable spacetime points.

II. TEST MASTER FIELDS

The discussion of the temporal test matrix is relatively simple, as the master field $\hat{\underline{A}}^0$ is assumed to have been diagonalized and ordered by an appropriate global gauge transformation [7]. This $N \times N$ traceless Hermitian test matrix is obtained as follows:

$$\hat{\underline{A}}_{\text{test}}^0 = \text{diag} \left[\bar{\alpha}(1), \dots, \bar{\alpha}(N) \right], \quad (1a)$$

$$\bar{\alpha}(i) = \tilde{\alpha}(i) - \frac{1}{N} \left(\sum_{j=1}^N \tilde{\alpha}(j) \right), \quad (1b)$$

$$\tilde{\alpha}(i) = \text{rand} \left[\frac{i-1}{N}, \frac{i}{N} \right], \quad (1c)$$

with $i \in \{1, \dots, N\}$ and $\text{rand}[x, y]$ giving a uniform pseudorandom real number in the interval $[x, y]$.

Next, we construct a test master field $\hat{\underline{A}}_{\text{test-1}}^1$ with a band-diagonal structure of width ΔN and average absolute values along the diagonal given by a parabola with approximate value 1 halfway ($i \sim N/2$) and approximate value 2 at the edges ($i = 1$ and $i = N$). Specifically, this $N \times N$ traceless Hermitian matrix with bandwidth ΔN (assumed to be even) is obtained as follows:

$$\hat{\underline{A}}_{\text{test-1}}^1 = \frac{1}{2} \left(\bar{A}^1 + \bar{A}^{1\dagger} \right) - \frac{1}{N} \text{tr} \left[\frac{1}{2} \left(\bar{A}^1 + \bar{A}^{1\dagger} \right) \right] \mathbb{1}_N, \quad (2a)$$

$$\left(\overline{A}^1\right)_{i,j} = \begin{cases} r_\chi \overline{x}^1(i), & \text{for } j - \Delta N/2 \leq i \leq j + \Delta N/2, \\ 0, & \text{otherwise,} \end{cases}, \quad (2b)$$

$$r_\chi = (1 - \chi) \text{rand}[-2, +2] + \chi \text{rand}[\pm 1], \quad (2c)$$

$$\overline{x}^1(i) = 1 + \left[\left(i - \frac{1}{2} \right) \frac{2}{N} - 1 \right]^2, \quad (2d)$$

$$\chi \in \{0, 1\}, \quad (2e)$$

with $\mathbb{1}_N$ the $N \times N$ identity matrix, indices i and j taking values in $\{1, \dots, N\}$, $\text{rand}[x, y]$ defined below (1c), and $\text{rand}[\pm 1]$ giving $+1$ with probability $1/2$ and -1 with probability $1/2$. The parameter χ distinguishes between a continuous or a discrete range for the randomized entries on the individual rows of the band diagonal of the matrix. The ‘‘expanding’’ behavior (2d), with a minimum at the halfway point, mimics the numerical results obtained in Refs. [3–5], assuming that \overline{x}^1 corresponds to one of the ‘‘large’’ dimensions of the $3 + 6$ split. The numerical results of these last references may, in fact, give a rough approximation of the genuine IIB-matrix-model master field (especially interesting are the $N = 128$ and $N = 192$ matrices obtained in Ref. [4]).

The analysis in the sections below will start from the test-1 master field (1) and (2), but, later, will also consider a test-2 master field $\widehat{A}_{\text{test-2}}^1$ with more structure. Roughly speaking, this test-2 master field again has a band-diagonal structure with parabolic behavior, but now there is also a finer modulation of $(2 \Delta N) \times (2 \Delta N)$ diagonal blocks, which alternately are reduced by a positive factor $\kappa < 1$ or boosted by a positive factor $\lambda > 1$, and a further modulation of $\Delta N \times \Delta N$ diagonal blocks, which alternately have $+1$ or -1 on the diagonal.

Assuming N , ΔN , and $N/\Delta N \equiv L$ all to be even integers, this $N \times N$ traceless Hermitian test matrix is given by the following expression:

$$\widehat{A}_{\text{test-2}}^1 = \frac{1}{2} \left(\widetilde{A}^1 + \widetilde{A}^{1\dagger} \right) - \frac{1}{N} \text{tr} \left[\frac{1}{2} \left(\widetilde{A}^1 + \widetilde{A}^{1\dagger} \right) \right] \mathbb{1}_N, \quad (3a)$$

$$\widetilde{A}^1 = D_{\kappa\lambda} \cdot D_{\text{pm}} \cdot \overline{A}^1, \quad (3b)$$

$$D_{\kappa\lambda} = \text{diag}[\kappa, \dots, \kappa, \lambda, \dots, \lambda, \dots, \lambda, \dots, \lambda], \quad (3c)$$

$$D_{\text{pm}} = \text{diag}[+1, \dots, +1, -1, \dots, -1, \dots, -1, \dots, -1], \quad (3d)$$

$$\left(\overline{A}^1\right)_{i,j} = \begin{cases} \overline{r}_\xi \overline{x}^1(i), & \text{for } j - \Delta N/2 \leq i \leq j + \Delta N/2, \\ 0, & \text{otherwise,} \end{cases}, \quad (3e)$$

$$\bar{r}_\xi = \text{rand}[1 - \xi, 1 + \xi], \quad (3f)$$

$$\bar{x}^1(i) = 1 + \left[\left(i - \frac{1}{2} \right) \frac{2}{N} - 1 \right]^2, \quad (3g)$$

$$0 < \kappa \leq 1 \leq \lambda, \quad (3h)$$

$$0 < \xi < 1, \quad (3i)$$

with $i, j \in \{1, \dots, N\}$ and $\text{rand}[x, y]$ defined below (1c). The real numbers κ and λ in (3c) are each repeated $2 \Delta N$ times [making for $L/2$ diagonal $(2 \Delta N) \times (2 \Delta N)$ blocks] and the real numbers $+1$ and -1 in (3d) are each repeated ΔN times [making for L diagonal $\Delta N \times \Delta N$ blocks].

The ± 1 fine-structure of (3d) is inspired by the similar fine-structure of an exact “classical” solution with $\Delta N \sim 1$ found in App. A of Ref. [6]. The *raison d’être* of the κ, λ fine-structure in (3c) will become clear in Sec. V. Remark also that the IIB-matrix-model variables are complex Hermitian, whereas the two test master fields of this section are real.

III. EXTRACTION PROCEDURE

The procedure for obtaining spacetime points from the master field has been outlined in Sec. IV of Ref. [7]. The basic idea is to consider, in each of the ten matrices \hat{A}^μ , the K blocks of size $n \times n$ centered on the diagonal. Here, we assume that $N = K * n$, for positive integers K and n , and that \hat{A}^0 has already been diagonalized and ordered by an appropriate global gauge transformation. The coordinates of the spacetime points are then obtained from the average of the eigenvalues in each $n \times n$ block. If the IIB-matrix-model master field \hat{A}^μ has a diagonal band width ΔN , we expect that n must be chosen to be approximately equal to ΔN or, better, significantly larger than ΔN . Furthermore, it is possible to introduce a length scale ℓ into the IIB matrix model, as discussed in Ref. [7], so that the bosonic matrix variable A^μ carries the dimension of length, as does the corresponding master field \hat{A}^μ . Throughout this article, we take length units which set $\ell = 1$.

The test master field \hat{A}_{test}^0 , as given by (1), then gives the following temporal coordinate:

$$\hat{x}^0(\sigma) \equiv \tilde{c} \hat{t}(\sigma) = \frac{1}{n} \sum_{l=1}^n \bar{\alpha}_{(k-1)n+l}, \quad (4)$$

for $\sigma \equiv k/K \in (0, 1]$ with $k \in \{1, \dots, K\}$ and $K = N/n$. The velocity \tilde{c} in (4) will be set to unity in the following. The temporal coordinate $\hat{t}^1(\sigma)$ takes values in the range $[-0.5, 0.5]$.

Similarly, the test-1 master field $\widehat{\underline{A}}_{\text{test-1}}^1$, as given by (2), gives the following coordinate in one spatial dimension:

$$\widehat{x}^1(\sigma) = \frac{1}{n} \sum_{l=1}^n \left[\overline{\beta}^1 \right]_{(k-1)n+l}, \quad (5)$$

for $\sigma \equiv k/K \in (0, 1]$ and eigenvalues $\overline{\beta}_i^1$ of the $n \times n$ blocks along the diagonal in the $N \times N$ matrix (2). The same expression (5) gives a spatial coordinate from the test-2 master field (3).

Before we start with the explicit calculation of the spacetime points (4) and (5) from our test master fields, we have a few general remarks on the adopted coarse-graining procedure. In order to cover the ΔN band diagonal of the master field completely, it would perhaps be better to let the $n \times n$ blocks, with $n > \Delta N$, overlap halfway. But, then, there would be the problem of double-counting some of the information contained in the master field and, moreover, there would be no way to obtain a clear ordering of the extracted information with respect to time. For these reasons, we prefer to keep, in our exploratory analysis, the simple procedure of having the $n \times n$ blocks touch on the diagonal, without overlap: even though the $n \times n$ block eigenvalues are not perfect (some information from the master field has been lost), there is a clear ordering of the average (5) with respect to the coordinate time t from (4).

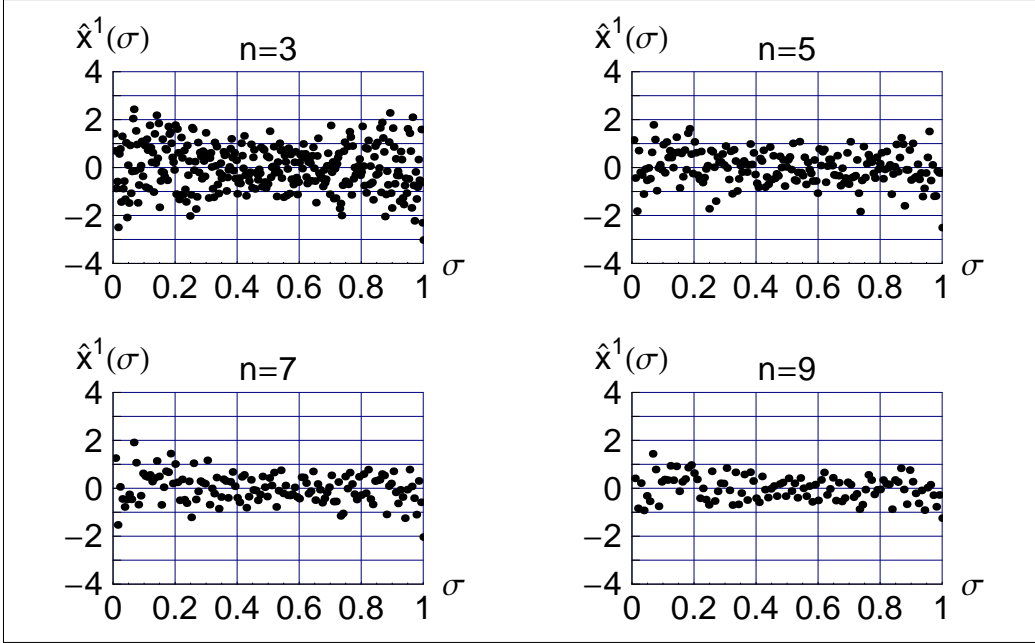
IV. SPACETIME POINTS FROM THE TEST-1 MASTER FIELD

Now, choose fixed values of N (assumed to be odd) and ΔN (assumed to be even) in the test master field $\widehat{\underline{A}}_{\text{test-1}}^1$ from (2) for $\chi = 0$. Then, for various choices of the block size n (which must be odd, because N has been assumed to be odd), the procedure from Sec. III gives the spatial coordinate $\widehat{x}^1(\sigma)$ from (5), for $\sigma \in (0, 1]$. Numerical results are presented in the upper panel-quartet of Fig. 1. All numerical results reported in this paper were obtained with MATHEMATICA 5.0 [8].

The calculation of the temporal coordinate is simpler, as the test master field $\widehat{\underline{A}}_{\text{test}}^0$ from (1) is already diagonal with explicit eigenvalues. The temporal coordinate $\widehat{t}(\sigma)$ follows from (4) for $\tilde{c} = 1$ and $\sigma \in (0, 1]$. It turns out that \widehat{t} is approximately linearly proportional to σ , as shown by the lower panel-quartet of Fig. 1. From these results we obtain $\widehat{x}^1(\widehat{t})$, as shown by Fig. 2.

For completeness, we also show, in Fig. 3, the results with discrete values ($\chi = 1$) on the rows of the band diagonal for $\Delta N = 4$, where the role of the χ parameter has been explained in the sentence starting below (2e). Similar $n = 3$ results have been obtained for $\Delta N = 2$ and $\Delta N = 6$.

$N=945, \Delta N=4, \chi=0$



$N=945, \Delta N=4$

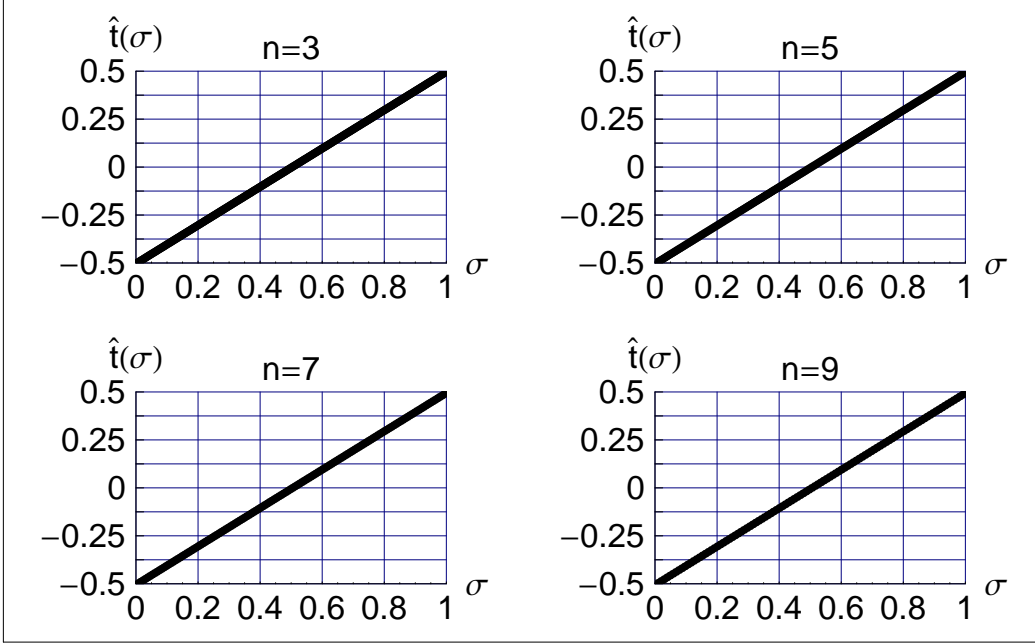


FIG. 1. The spatial coordinate $\hat{x}^1(\sigma)$, for $\sigma \in (0, 1]$, is shown in the upper panel-quartet. This coordinate $\hat{x}^1(\sigma)$ is obtained by the procedure of Sec. III applied to the test-1 master field $\hat{A}_{\text{test-1}}^1$ as given by (2), for matrix size $N = 3*5*7*9 = 945$, band-diagonal width $\Delta N = 4$, and parameter $\chi = 0$ to select a continuous range of values on the individual rows of the band diagonal of the matrix. The temporal coordinate $\hat{t}^1(\sigma)$, obtained by applying the same procedure to the matrix (1), is shown in the lower panel-quartet. Eliminating σ between $\hat{x}^1(\sigma)$ and $\hat{t}^1(\sigma)$ gives $\hat{x}^1(\hat{t})$, which is shown in Fig. 2.

$N=945, \Delta N=4, \chi=0$

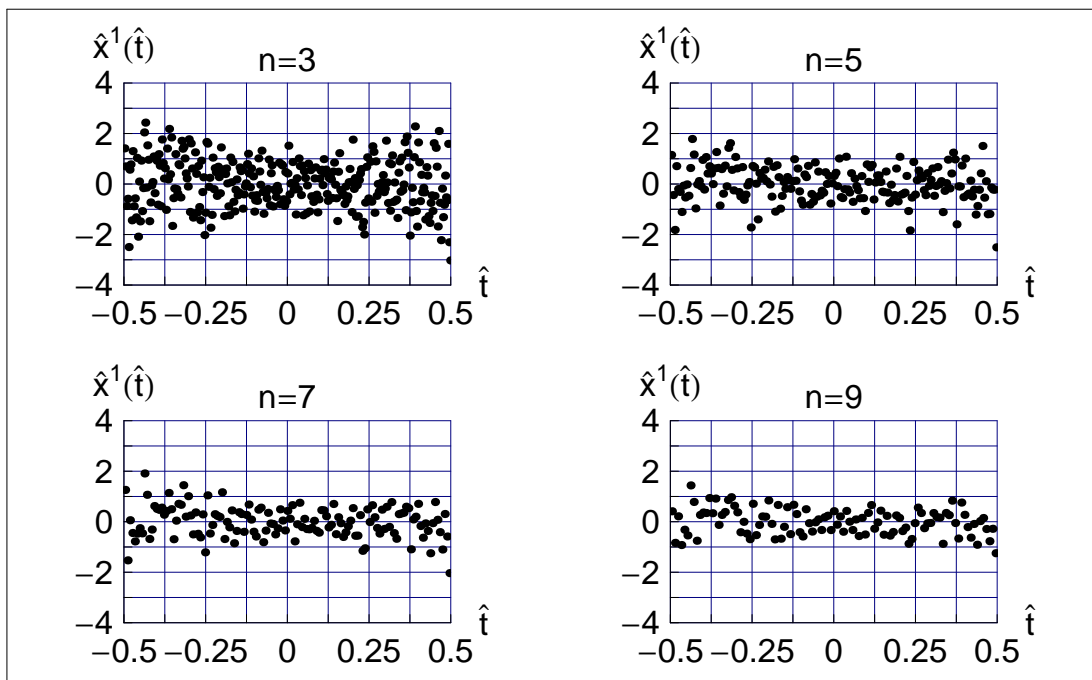


FIG. 2. Behavior of \hat{x}^1 versus \hat{t} from the test-1 results of Fig. 1.

$N=945, \Delta N=4, \chi=1$

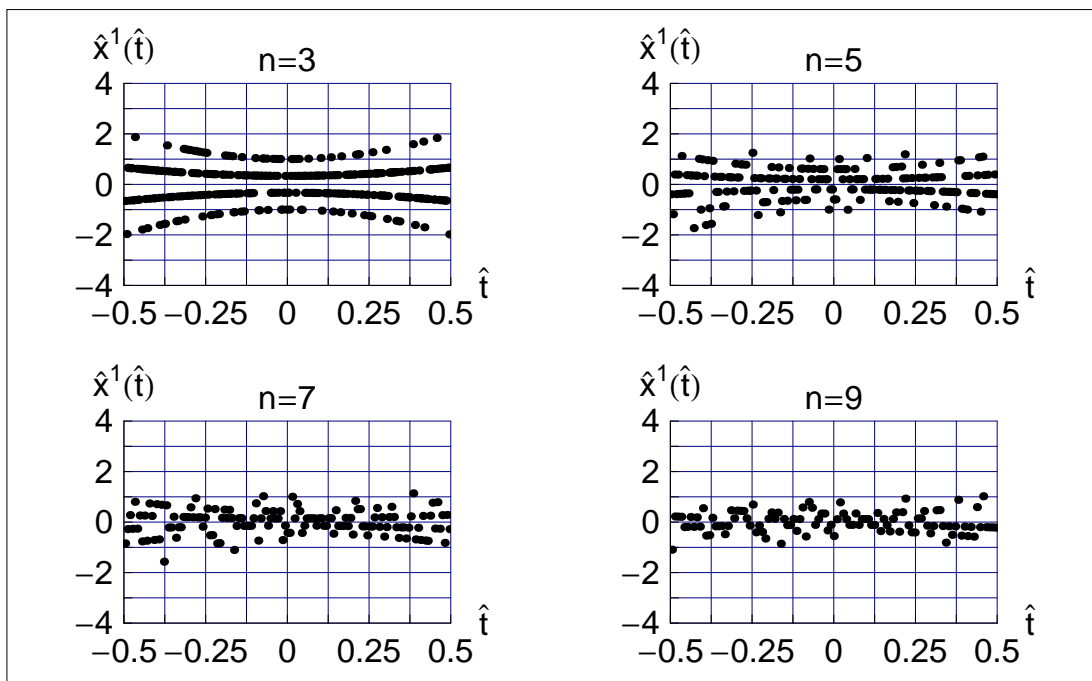


FIG. 3. Same as Fig. 2, but the test-1 master field (2) now has parameter $\chi = 1$ to select a discrete range of values on the individual rows of the band diagonal of the matrix.

$N=768$, $\Delta N=4$, $\kappa=\lambda=1$, $\xi=0$

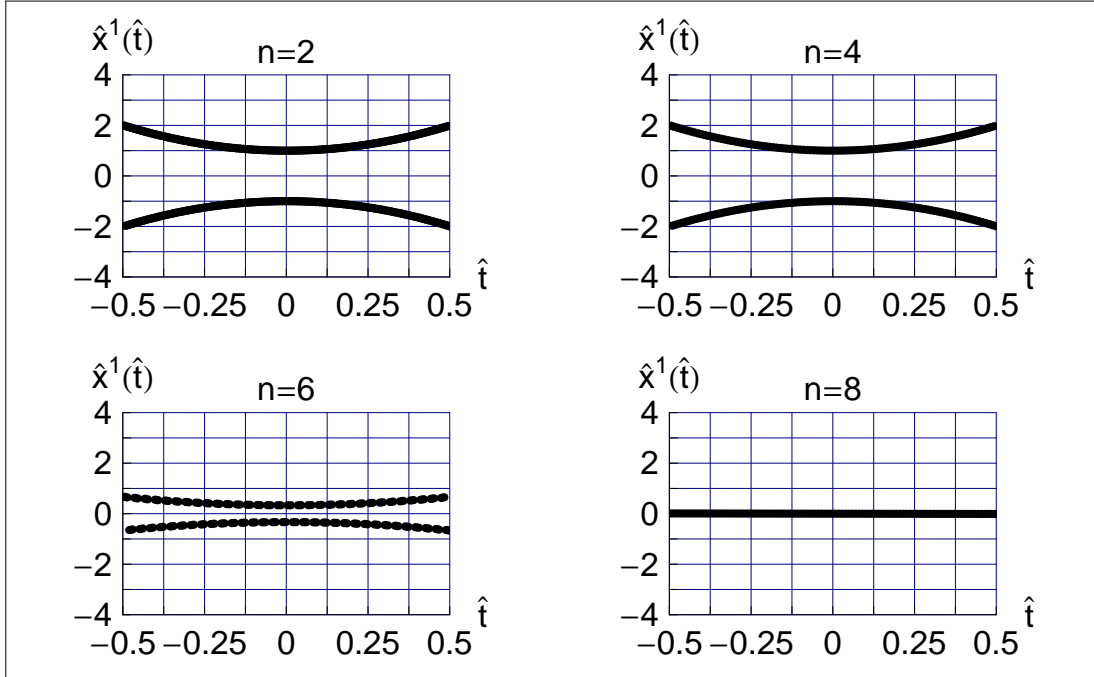


FIG. 4. Behavior of \hat{x}^1 versus \hat{t} from the test-2 master field (3), for $N = 2^8 * 3 = 768$ and $\Delta N = 4$, and with trivial modulation parameters, $\kappa = \lambda = 1$, and vanishing randomization parameter, $\xi = 0$.

$N=768, \Delta N=4, \kappa=1/2, \lambda=3/2, \xi=0$

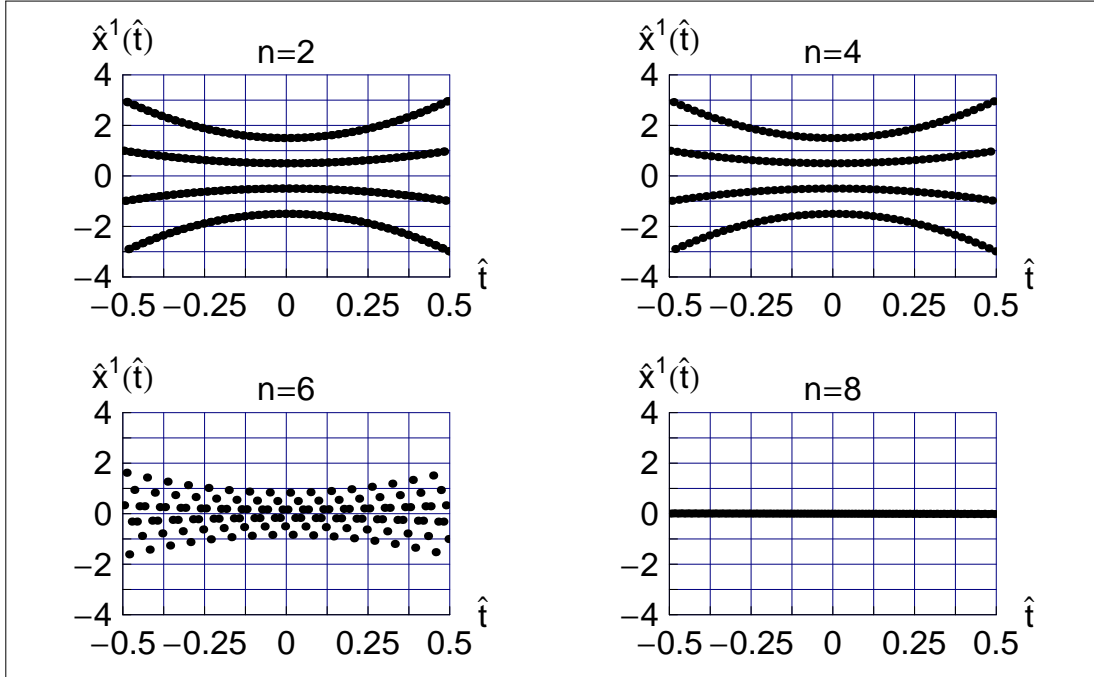


FIG. 5. Same as Fig. 4, but now with nontrivial modulation parameters, $\kappa = 1/2$ and $\lambda = 3/2$.

$N=768, \Delta N=4, \kappa=1/2, \lambda=3/2, \xi=1/5$

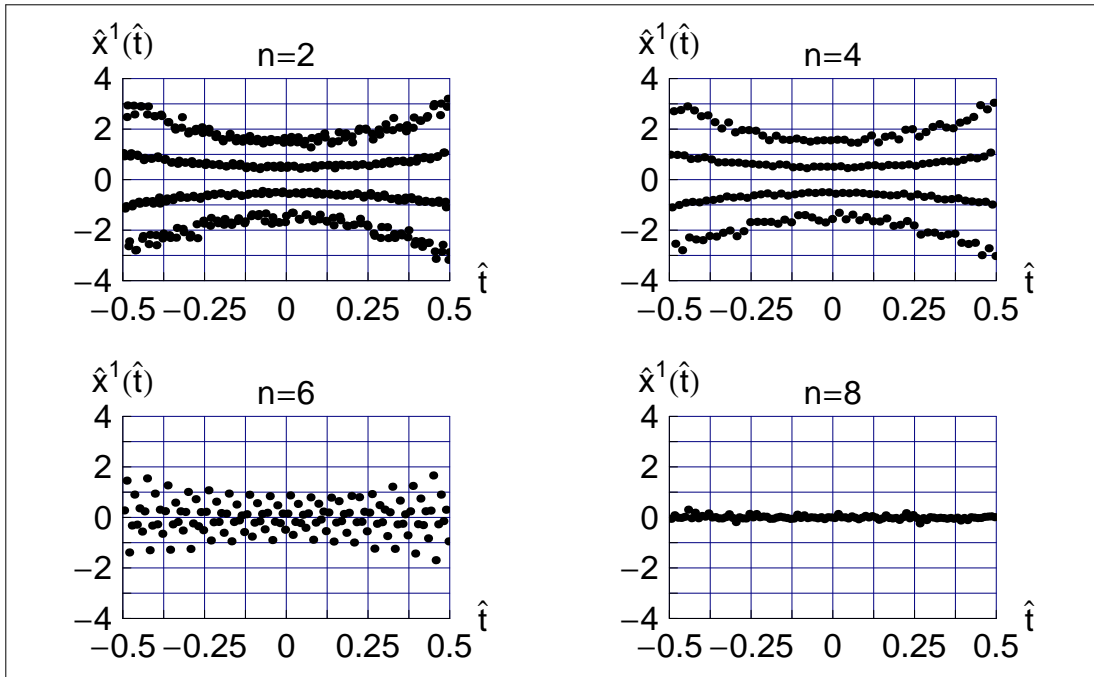


FIG. 6. Same as Fig. 5, but now with a nonvanishing randomization parameter, $\xi = 0.2$.

V. SPACETIME POINTS FROM THE TEST-2 MASTER FIELD

The $n = 3$ results of Fig. 2 perhaps show a point set expanding with time $|t|$, but it is not clear if a classical spacetime emerges with an expanding *volume* (at this moment, we do not have the metric distance between the points). In that sense, the $n = 3$ results of Fig. 3 may be more promising, as they *suggest* four “strands” of spacetime separating from each other as $|t|$ increases (we are using “strand” in the meaning of a “strand of pearls”). Incidentally, a somewhat related pattern has been observed in Fig. 5 of Ref. [5].

Returning to the strands of Fig. 3, the following question arises: is it at all possible to *design* a special master field $\hat{\mathbf{A}}_{\text{special}}^1$, so that the procedure of Sec. III gives *multiple* strands of spacetime, which fill out an expanding universe?

The answer is affirmative and an example for up to four spacetime strands is given by the test-2 matrix (3). For $\kappa = \lambda = 1$, we get two strands (Fig. 4) and, for $\kappa = 1/2$ and $\lambda = 3/2$, for example, we get four strands with $n = 2$ and $n = 4$ averaging (Figs. 5 and 6); the $n = 6$ results of Fig. 5 even suggest the presence of six strands. It appears possible to get more than four (or six) spacetime strands by introducing even more parameters and structure along the diagonal of the test matrix.

The next outstanding task is to obtain the emergent metric and to calculate the metric distances between points on a single strand and between points on different strands. At this moment, we have no solid results but only some speculative remarks. One speculative remark is that, for two strands extending in two “large” spatial dimensions, two “neighboring” points on a single strand may have a smaller metric distance than two “neighboring” points on different adjacent strands. Appendix A reports on a toy-model calculation which suggests such a result.

VI. DISCUSSION

In this somewhat technical paper, we have considered several test matrices and obtained tentative spacetime points by applying the procedure of Ref. [7] to these matrices. These test matrices have a band-diagonal structure, one being strictly diagonal to represent the time coordinate t and another having a finite bandwidth ΔN to represent a typical spatial coordinate x^1 from a “large” dimension, whose average absolute value $|x^1|$ grows quadratically with t (a behavior seen in the numerical results of Refs. [3–5]). The hope is that these test matrices may help us to understand a possible fine-structure of the genuine IIB-matrix-model master field.

As a first step towards such an understanding, we have constructed the test-2 matrix from (3), which has a very special fine-structure to allow for the appearance of multiple “strands” of spacetime (Figs. 4–6). In fact, this understanding allows us to interpret the

somewhat surprising $n = 3$ and $n = 5$ results of Fig. 3, which indicate the appearance of, respectively, four and six strands (with some good will, the $n = 7$ results can be seen to hint at the presence of eight strands). The heuristic idea, now, is that the simple flip-flop behavior on each row of the matrix gives a repeating pattern if a sufficiently large number of rows is considered ($N \rightarrow \infty$). Preliminary numerical results extending the calculation of Fig. 3 appear to confirm the appearance of more than six strands.

Many questions remain as to the procedure for the extraction of the spacetime points, not to mention the spacetime metric. But even more important, at this moment, is to obtain a *reliable* approximation of the IIB-matrix-model master field, which may or may not display some form of fine-structure.

Appendix A: Toy-model calculation of metric distances

In this appendix, we report on a toy-model calculation which extends a similar calculation presented in Sec. V of Ref. [7].

Start from the emergent inverse metric as given by (5.1) of Ref. [7] (based on an earlier expression from Ref. [2]):

$$g^{\mu\nu}(x) \sim \int d^{10}y \langle\langle \rho(y) \rangle\rangle (x-y)^\mu (x-y)^\nu f(x-y) r(x,y), \quad (\text{A1})$$

where $\langle\langle \rho(x) \rangle\rangle$ is the average density function of emergent spacetime points, $r(x,y)$ is the correlation function from these density functions, and $f(x-y)$ is a correlation function that appears in the effective action of a low-energy scalar degree of freedom; see Refs. [2, 7] for further details.

Consider a simple setup in the (x^2, x^3) plane with two finite bands B_+ and B_- (Fig. 7),

$$B_+ = \{(x^2, x^3) \mid x^2 \in [-2, 2], x^3 \in [+1 - \Delta x/2, +1 + \Delta x/2]\}, \quad (\text{A2a})$$

$$B_- = \{(x^2, x^3) \mid x^2 \in [-2, 2], x^3 \in [-1 - \Delta x/2, -1 + \Delta x/2]\}, \quad (\text{A2b})$$

$$0 < \Delta x/2 < 1, \quad (\text{A2c})$$

where the bands may be thought to arise from wiggly strands such as shown by the $n = 4$ results of Fig. 6. The average density of emerging spacetime points is assumed to be nonvanishing only over these bands,

$$\langle\langle \rho(x) \rangle\rangle = \begin{cases} 1/\ell^{10}, & \text{for } (x^2, x^3) \in B_+ \cup B_-, \\ 0, & \text{otherwise,} \end{cases}, \quad (\text{A3})$$

with ℓ the length scale of the IIB matrix model and all coordinates x^μ carrying the dimension of length, as discussed in Sec. III. The length units of the setup in Fig. 7 are assumed to correspond to $\ell = 1$.

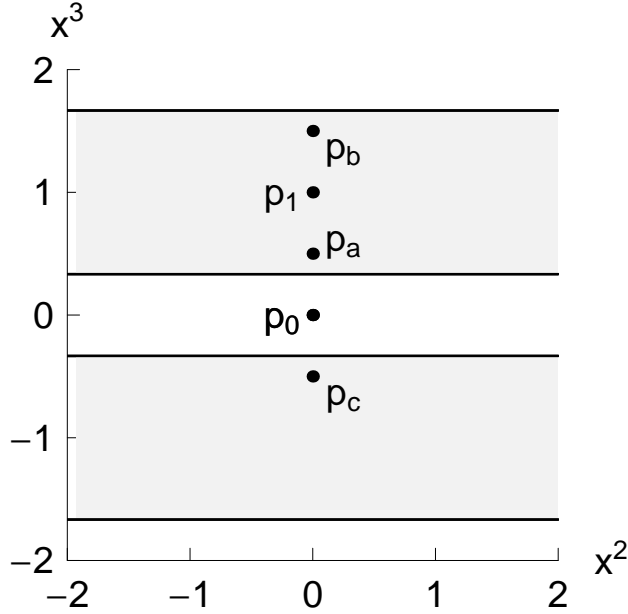


FIG. 7. Setup for the toy-model calculation, where the shaded areas indicate the bands B_{\pm} (centered on $x^3 = \pm 1$ and having widths $\Delta x = 4/3$) over which spacetime points emerge. Metric components at two points p_0 and p_1 are compared and metric distances between three further points p_a , p_b , and p_c calculated.

Next, restrict (A1) to two spatial dimensions (with coordinates x^2 and x^3) and introduce a symmetric cutoff on the integrals at ± 2 , while making two further simplifications,

$$f(x) = 1/\ell^2, \quad (\text{A4a})$$

$$r(x, y) = 1, \quad (\text{A4b})$$

with $\ell = 1$ for the chosen length units. Note that the assumptions (A4) perhaps make sense if the space patch considered is sufficiently small in physical units; see also the discussion below for another setup.

It is, now, straightforward to calculate the inverse metric components g^{22} , g^{33} , and $g^{23} = g^{32}$ from (A1) for two points p_0 and p_1 (Fig. 7) with the following coordinates:

$$(x^2, x^3)_{p_0} = (0, 0), \quad (\text{A5a})$$

$$(x^2, x^3)_{p_1} = (0, 1), \quad (\text{A5b})$$

so that point p_1 lies in the upper band B_+ and point p_0 between the bands B_+ and B_- . As the y^3 integral in (A1) is elementary, we obtain immediately

$$0 < g^{33}(p_0) < g^{33}(p_1), \quad (\text{A6a})$$

$$0 < g^{22}(p_0) = g^{22}(p_1), \quad (\text{A6b})$$

$$0 = g^{23}(p_0) = g^{23}(p_1). \quad (\text{A6c})$$

We actually need the metric $g_{\mu\nu}(x)$ for calculating the metric distances (from $ds^2 = g_{\mu\nu} dx^\mu dx^\nu$) and we have the following inequalities and equalities from (A6):

$$g_{33}(p_0) > g_{33}(p_1) > 0, \quad (\text{A7a})$$

$$g_{22}(p_0) = g_{22}(p_1) > 0, \quad (\text{A7b})$$

$$g_{23}(p_0) = g_{23}(p_1) = 0. \quad (\text{A7c})$$

The results (A6) and (A7) extend to other points \bar{p}_1 with $x^2 = 0$ lying in the band B_+ and other points \bar{p}_0 with $x^2 = 0$ lying between the bands B_+ and B_- . In fact, the metric component $g_{33}(x^2, x^3)$ at $x^2 = 0$ is a positive symmetric function of x^3 having a maximum at $x^3 = 0$ and dropping monotonically with $|x^3|$,

$$g_{33}(0, |x^3|) > g_{33}(0, |x^{3'}|) > 0, \quad \text{for } 0 < |x^3| < |x^{3'}|. \quad (\text{A8})$$

The results (A7a) and (A8) are definitely surprising, with a larger metric component g_{33} in the “empty space” between the bands than in the bands themselves. These results trace back to the quadratic behavior of the $\mu = \nu = 3$ integrand in (A1), as there is no damping from the remaining factors $f(x - y)$ and $r(x, y)$, according to assumptions (A4).

A different setup has (A4a) replaced by, for example,

$$f(x) = \ell^2 / [\ell^4 + (x^2)^2], \quad (\text{A9})$$

with $x^2 \equiv \eta_{\mu\nu} x^\mu x^\nu$ in terms of the “coupling constants” $\eta_{\mu\nu}$ from the Lorentzian IIB matrix model. In length units with $\ell = 1$, the *Ansatz* (A9) simply reads $f(x) = 1/(1 + x^4)$. This alternative setup gives the inequality $g_{33}(p_0) < g_{33}(p_1)$, which corresponds to having a smaller metric component g_{33} in the “empty space” between the bands than in the bands themselves. Moreover, the actual value of $g_{33}(p_0)$ obtained from this setup with $f(x) = 1/(1 + x^4)$ is generically larger than the value obtained from the original setup with $f(x) = 1$. This larger value of g_{33} is simply due to the reduction of the $\mu = \nu = 3$ integrand (A1) by the function $f(x) = 1/(1 + x^4)$, making for a smaller value of g^{33} and, hence, a larger value of g_{33} (the same argument applies to the g_{22} component). A straightforward calculation of the squared distance between the points p_0 and p_1 gives, in fact, a larger value from the setup with $f(x) = 1/(1 + x^4)$ than from the setup with $f(x) = 1$, all other assumptions being equal. Together with the above parenthetical remark on the g_{22} component, we then find that the space patch from the setup with $f(x) = 1/(1 + x^4)$ is larger than the space patch from the setup with $f(x) = 1$.

Returning to the original setup with assumptions (A4), we like to give an explicit example and take the following numerical value of the bandwidth:

$$\Delta x = 4/3, \quad (\text{A10})$$

and consider the following three points p_a , p_b , and p_c (Fig. 7) with coordinates:

$$(x^2, x^3)_{p_a} = (0, 1/2), \tag{A11a}$$

$$(x^2, x^3)_{p_b} = (0, 3/2), \tag{A11b}$$

$$(x^2, x^3)_{p_c} = (0, -1/2), \tag{A11c}$$

so that p_a and p_b lie on the single band B_+ and p_c on the other band B_- . The coordinate distance between p_a and p_b equals the coordinate distance between p_a and p_c . But, from (A8), we obtain different metric distances between these two pairs of points:

$$0 < d(p_a, p_b) < d(p_a, p_c) . \tag{A12}$$

If all assumptions hold true (possibly for a relatively small region of spacetime), the result (A12) would imply that two spatially-separated neighboring points on a single band have a smaller metric distance than two spatially-separated neighboring points on different adjacent bands.

-
- [1] N. Ishibashi, H. Kawai, Y. Kitazawa, and A. Tsuchiya, “A large- N reduced model as superstring,” Nucl. Phys. B **498**, 467 (1997) arXiv:hep-th/9612115.
 - [2] H. Aoki, S. Iso, H. Kawai, Y. Kitazawa, A. Tsuchiya, and T. Tada, “IIB matrix model,” Prog. Theor. Phys. Suppl. **134**, 47 (1999), arXiv:hep-th/9908038.
 - [3] S.W. Kim, J. Nishimura, and A. Tsuchiya, “Expanding (3+1)-dimensional universe from a Lorentzian matrix model for superstring theory in (9+1)-dimensions,” Phys. Rev. Lett. **108**, 011601 (2012), arXiv:1108.1540.
 - [4] J. Nishimura and A. Tsuchiya, “Complex Langevin analysis of the space-time structure in the Lorentzian type IIB matrix model,” JHEP **1906**, 077 (2019), arXiv:1904.05919.
 - [5] K. Hatakeyama, A. Matsumoto, J. Nishimura, A. Tsuchiya, and A. Yosprakob, “The emergence of expanding space-time and intersecting D-branes from classical solutions in the Lorentzian type IIB matrix model,” Prog. Theor. Exp. Phys. **2020**, 043B10 (2020), arXiv:1911.08132.
 - [6] F.R. Klinkhamer, “On the emergence of an expanding universe from a Lorentzian matrix model,” arXiv:1912.12229.
 - [7] F.R. Klinkhamer, “IIB matrix model: Emergent spacetime from the master field,” arXiv:2007.08485.
 - [8] S. Wolfram, *Mathematica: A System for Doing Mathematics by Computer, Second Edition* (Addison-Wesley, Redwood City, CA, 1991).